

The original publication is available at <http://cercor.oxfordjournals.org>
via the following DOI: <http://dx.doi.org/10.1093/cercor/bhq108>

Neuroanatomical Prerequisites for Language Functions in the Maturing Brain

Jens Brauer*, Alfred Anwander and Angela D. Friederici

Max Planck Institute for Human Cognitive and Brain Sciences, Leipzig, Germany

***Corresponding Author:**

Dr Jens Brauer

Max Planck Institute for Human Cognitive and Brain Sciences

Stephanstrasse 1a

04103 Leipzig, Germany

<http://www.cbs.mpg.de/~brauer>

Preprint submitted to Cerebral Cortex.

Final draft: June 2010

Key words:

development, DTI, fiber tractography, fMRI, language

Abstract

The 2 major language-relevant cortical regions in the human brain, Broca's area and Wernicke's area, are connected via the fibers of the arcuate fasciculus/superior longitudinal fasciculus (AF/SLF). Here, we compared this pathway in adults and children and its relation to language processing during development. Comparison of fiber properties demonstrated lower anisotropy in children's AF/SLF, arguing for an immature status of this particular pathway with conceivably a lower degree of myelination. Combined diffusion tensor imaging (DTI) data and functional magnetic resonance imaging (fMRI) data indicated that in adults the termination of the AF/SLF fiber projection is compatible with functional activation in Broca's area, that is pars opercularis. In children, activation in Broca's area extended from the pars opercularis into the pars triangularis revealing an alternative connection to the temporal lobe (Wernicke's area) via the ventrally projecting extreme capsule fiber system. fMRI and DTI data converge to indicate that adults make use of a more confined language network than children based on ongoing maturation of the structural network. Our data suggest relations between language development and brain maturation and, moreover, indicate the brain's plasticity to adjust its function to available structural prerequisites.

Introduction

Language is a unique human capacity but its development in the brain remains largely unexplained. Functional imaging studies in adults show that sentence comprehension is supported by a frontotemporal network (Friederici 2002; Hashimoto and Sakai 2002; Hickok and Poeppel 2007; Tyler and Marslen-Wilson 2008). The processing of grammatical structures involves Broca's area, in particular Brodmann Area (BA) 44 (Friederici, Bahlmann, et al. 2006) and the posterior portion of Wernicke's area (Bornkessel et al. 2005) and a dynamic interplay between these 2 areas (Snijders et al. 2009). These 2 language relevant brain regions are connected by fiber bundles that guarantee information transmission. There seem to be substantial phylogenetic differences in the white matter fiber pathways that connect the cortical circuits underlying language functions in humans. Structural brain imaging data suggest distinctions between human and nonhuman primates in

fiber tracts connecting the frontal and temporal brain areas. By combining microelectrode recording with anatomical tract tracing, 2 functionally different pathways have been defined in the macaque, these being a dorsal and a ventral route that connect the auditory cortex to the prefrontal cortex (Romanski et al. 1999). Data revealed a ventral pathway running from the inferior frontal gyrus (IFG) and insular cortex to the superior temporal gyrus and sulcus (STG/STS) as the dominant pathway in the macaque, whereas a dorsal pathway from BA 44, 45, and 47 in the IFG to the posterior STG/STS and the middle temporal gyrus is dominant in humans (Rilling et al. 2008). Nevertheless, both pathway connections are existent in the human brain (Frey et al. 2008; Saur et al. 2008; Hua et al. 2009). The dorsal pathway (Friederici, Bahlmann, et al. 2006; Rilling et al. 2008) is argued as a critical language-relevant connection between the 2 brain regions that have been shown to support the processing of syntactically complex sentences (Constable et al. 2004; Bornkessel et al. 2005). Others take the ventral pathway to be the crucial one for language comprehension (Saur et al. 2008). The distinctive contributions of this dorsal and the ventral pathways to language functions thus are still a matter of debate (Friederici 2009a, 2009b; Weiller et al. 2009).

Phylogenetic arguments derived from cross-species comparisons are important but can only contribute indirectly to our understanding of the human language faculty (Ghazanfar 2008; Petkov et al. 2009). An alternative route toward achieving more profound comprehension of the brain basis of human language can be taken by simultaneously investigating ontogenetic development of brain structures and brain functions of language in humans. The exact location and extent of human white matter fiber pathways can be identified noninvasively in vivo by means of diffusion tensor imaging (DTI). Based on structural properties of the tissue, DTI measures water diffusion in the brain as well as its directional orientation (fractional anisotropy, FA) and thus provides useful information about the anatomy of the brain's fiber pathways. Furthermore, DTI allows the explicit assessment of changes in white matter maturation during ontogeny.

Structural maturation of fiber pathways in the brain is particularly characterized by increasing myelination of fibers, which is reflected in DTI by an increase in FA during infancy and childhood (Mukherjee et al. 2001; Barnea-Goraly et al. 2005; Dubois et al. 2008, Lebel et al. 2008). The process of initial myelination during human development is most pronounced before the second year of life, but further condensation and agglomeration continue (Lenroot

and Giedd 2006). These structural changes are accompanied by concurrent major developmental changes in motor, sensory, executive, and cognitive functions.

The development of language functions is still under investigation. Behavioral data, for example, indicate that the processing of syntactically complex sentences in particular, that is, sentences with a noncanonical word order, occurs late. It has been demonstrated that object-first sentences (Dittmar et al. 2008) or passive sentences (Hahne et al. 2004) are not fully understood before about age 7 years. From functional magnetic resonance imaging (fMRI) data in adults, we know that the processing of noncanonical sentences recruit Broca's area (Stromswold 1996; Rogalsky et al. 2008), in particular BA 44, and the posterior STG/STS (Bornkessel et al. 2005; Friederici, Fiebach, et al. 2006): 2 brain regions that are connected via the dorsal pathway (Catani et al. 2005; Rilling et al. 2008). Our knowledge concerning the functional neuroanatomy of language during development is still sparse. For auditory language comprehension, pediatric fMRI data revealed functional and causal connectivity between frontal and temporal regions (Wilke et al. 2009). Stronger activation in the language relevant areas and beyond these for children compared with adults has been reported for sentence processing (e.g., Gaillard et al. 2000; Brauer and Friederici 2007). However, the pattern of development of functional brain activation seems complex including increases and decreases of functional activation across brain regions during development (Rivera et al. 2005; Schlaggar and Church 2009) and a fine tuning and/or focalization of activation in task relevant areas (Casey et al. 2005; Cohen Kadosh and Johnson 2007).

Here, we hypothesized that the human ability to successfully process sentences including their inherent grammatical and semantic information might require a strong and fully developed dorsal connection via the arcuate fasciculus/superior longitudinal fasciculus (AF/SLF) associating Broca's area to the posterior portion of the temporal cortex. DTI data were acquired from 7-year-old children and adults to identify brain regions of ongoing maturation in language-relevant areas by directly comparing fiber tract anatomy. Additionally, fMRI data on a well-established language comprehension paradigm were acquired to identify the brain areas that support auditory sentence processing in children and adults (Brauer and Friederici 2007; Brauer et al. 2008). A combined analysis of fMRI and DTI data converged functional and structural data.

Materials and Methods

Participants

Seven-year-old children, recruited from local kindergartens by open letter, participated in the study. Interested parents were invited for an informative meeting about the experiment and procedures. They gave written informed consent, and children gave verbal assent prior to assessment and scanning. Data from 12 children were obtained, 2 of which had to be excluded from further analysis due to movement in the scanner during data acquisition. Thus, data of 10 children (5 girls) were available (mean age 7.0 years, standard deviation [SD] 1.1, range 5.6-8.7). Additionally, 10 adults (5 females, mean age 27.8 years, SD 2.7, range 24.4-32.4) participated in the study after informed consent. No participant had any history of linguistic, neurological, or psychiatric disorders. Adult participants were students. Children were checked for typical development in intellectual and language abilities. They scored within the normal range on a nonverbal IQ test (Kaufman-Assessment Battery for Children, Kaufman and Kaufman 1994) at $IQ = 104.10$ (SD 11.41), a syntactic/semantic subscale of a language ability test (Heidelberger Sprachentwicklungstest, Grimm and Schoeler 1991) at $T = 55.20$ (5.14), and the Child Behavior Checklist (Achenbach 1998) at $T = 50.11$ (5.37) (IQ and T scores represent normalized test values as a projection onto an (age matched) reference population described by a mean IQ of 100 [SD 15] and a mean T of 50 [SD 10]). All participants were right handed and German native speakers. Protocols and procedures were approved by the Research Ethics Committee of the University of Leipzig.

Materials

Stimulus material consisted of short German sentences in the active voice from an established paradigm (Brauer and Friederici 2007; Brauer et al. 2008). The material included correct and incorrect basic sentences (e.g., “The frog croaks,” “The lion in the zoo roars,” “The yoghurt in tastes good,” or “The stone bleeds”). Participants evaluated each sentence by an acceptability judgment via button press.

For the purpose of auditory presentation, items were spoken by a trained female native speaker in a well-pronounced, child-directed manner. All sentences were recorded and digitized at 44.1 kHz, 16-bit mono. They had an average length of approximately 2 s. For adults, the session contained 200 trials plus 25 null events, in which the blood oxygen level--

dependent response was allowed to return to baseline state (Burock et al. 1998). For children, the session contained 120 trials plus 15 null events. In all other ways, the procedure was the same as that used for adults. Trials were presented every 8 s in a single session. In order to rule out any effect of experiment length, a shorter experiment in adults was simulated post hoc by truncating adults' data sets after 135 volumes. There were no relevant changes in activation results, particularly not for activation in Broca's area. Thus, length of experiment could not account for group differences in functional activation.

While listening to stimuli and during the entire measurement, participants could see a aquarium screensaver with fishes swimming calmly across the scene. In order to obtain increased signal-to-noise ratio, no distinction between syntactic and semantic information processing was made. Rather, language stimulation in general was contrasted against resting baseline (null events) since our main interest was general sentence processing (Brauer et al. 2008). Only correctly answered trials entered subsequent analyses.

Magnetic Resonance Imaging

fMRI and DTI data were acquired in separate sessions on a whole-body 3-T Magnetom Trio scanner (Siemens). Diffusion-weighted data and high-resolution *T1*-weighted images were obtained with an 8-channel head array coil. Diffusion-weighted images were obtained with a twicerefocused spin echo-planar-imaging (EPI) sequence (Reese et al. 2003), time echo (TE) 100 ms, time repetition (TR) 12 s, 128 x 128 image matrix, and field of view (FOV) 220 x 220 mm², providing 60 diffusion-encoding gradient directions with a b value of 1000 s/mm². Seven images without any diffusion weighting were obtained at the beginning of the scanning sequence and after each block of 10 diffusion-weighted images as anatomical reference for off-line motion correction. The interleaved measurement of 72 axial slices with 1.7-mm thickness (no gap) covered the entire brain. Random noise in the data was reduced by averaging three acquisitions. Additionally, fat saturation was employed together with 6/8 partial Fourier imaging, Hanning window filtering, and parallel acquisition (generalized autocalibrating partially parallel acquisitions with reduction factor 2).

For functional measurements, a gradient-echo EPI sequence was applied (TE 30ms, flip angle 90°, TR 2 s, bandwidth 100 kHz, matrix 64 x 64 voxels, FOV 192 mm, in-plane resolution 3 x 3 mm) for 20 slices (slice thickness 4 mm, 1 mm gap). *T1*-weighted modified driven equilibrium Fourier transform images (Ugurbil et al. 1993), matrix 256 x 256, TR 1.3 s, TE

7.4 ms, with a nonslice-selective inversion pulse followed by a single excitation of each slice (Norris 2000) were used for registration. For anatomical data, a *TI*-weighted 3D magnetization-prepared rapid gradient echo sequence was obtained with magnetization preparation consisting of a nonselective inversion pulse (TI 650 ms, TR 1.3 s, snapshot FLASH 10 ms, TE 3.97 ms, angle 10, bandwidth 67 kHz, matrix 256 3 240, slab thickness 192 mm, sagittal orientation, spatial resolution 1 x 1 x 1.5 mm). To avoid aliasing, oversampling was performed in read direction (head-foot).

Data Analysis

Data were processed using the software packages LIPSIA (Lohmann et al. 2001) and FSL (Smith et al. 2004). *TI*-weighted structural scans were used for skull stripping, and the brain images were then coregistered into Talairach space (Talairach and Tournoux 1988). Twenty-one images without diffusion weighting distributed over the entire sequence were used to estimate motion correction parameters using rigid-body transformations (Jenkinson et al. 2002). Motion correction for the 180 diffusion-weighted images was combined with a global registration to the *TI* anatomy computed using the same method. The gradient direction for each volume was corrected using the rotation parameters. The registered images were interpolated to the new reference frame with an isotropic voxel resolution of 1 mm, and the three corresponding acquisitions and gradient directions were averaged. Finally, for each voxel, a diffusion tensor was fitted to the data.

Classical methods such as voxel-wise analysis of DTI data can be affected by limitations, particularly in the context of investigations into brain maturation. The registration method may be restricted in its accuracy by low-dimensional transformations and the heterogeneity of signal intensities in FA maps. Image smoothing and statistical thresholding are further sources of artifacts (Jones et al. 2005). Therefore, in the present study tract-based spatial statistics (TBSS) were applied that allows for the registering of data sets onto the core white matter of one common target image (Smith et al. 2006).

A skeletonization algorithm that defined a group template for white matter tracts was applied, and normalized individual maps were projected onto this template. Skeletonization was employed for cerebral white matter without the cerebellum and thalamus. The cerebellum was omitted since it was not entirely included in the FOV region during scanning. The thalamus was likewise omitted, as this structure is an intermingled mixture of gray matter

nuclei and smaller white matter structures, and the focus of the study was the main fiber tract pathways in cerebral white matter, particularly frontotemporal connections.

Voxelwise statistic on the white matter skeleton was used, and correction for multiple comparisons across voxels was realized by permutation testing generating corrected cluster-based P values. Clusters of $P < 0.05$ were regarded as differing significantly between groups.

Anatomical connectivity and fiber orientation in human brain white matter was investigated by fiber tracking to compute the connectivity between cortical brain areas from the diffusion tensor maps (Anwander et al. 2007). Mean DTI data averaged for each group were examined by a whole-brain deterministic fiber tracking. The measured diffusion images for each group were aligned by nonlinear registration and combined to one data set. A diffusion tensor was fitted to the combined data resulting in one averaged diffusion tensor of each voxel in each group. In that way, the averaging is integrated implicitly in the tensorfitting procedure to avoid averaging of diffusion tensors. The reconstruction algorithm used the entire diffusion tensor to deflect the estimated fiber trajectory (Lazar et al. 2003) as implemented in MedINRIA according to Fillard et al. (2007). Fiber trajectories were started in all voxels (voxel size: 1 mm^3) with a $FA > 0.13$. All fibers crossing a seed volume were selected as white matter connections for a single seed point.

T1 images were normalized on a common source space, and motion artifacts were ruled out to contribute to any group differences in functional or diffusion results (see Supplementary Material). Statistical evaluation of functional activation was based on a general linear regression with prewhitening (Worsley et al. 2002). Autocorrelation parameters were estimated from the least squares residuals using Yule-Walker equations. These parameters were subsequently used to whiten both data and design matrix. Finally, the linear model was re-estimated using least squares on the whitened data to produce estimates of effects and their standard errors. The design matrix was generated with a synthetic hemodynamic response function (Josephs et al. 1997; Friston et al. 1998) and its first and second derivatives. Motion correction parameters and stimulus duration were included as regressors. For each participant, one contrast image was generated to represent the main effect of sentence presentation versus baseline. Individual functional data sets were aligned with the stereotactic reference space.

Single-participant contrast images were entered into a second-level random-effects analysis consisting of a 1-sample *t*-test across the contrast images of all subjects to indicate whether observed differences between conditions differed significantly from zero. Subsequently, *t* values were transformed into *z* scores. Group maps were thresholded at $z > 3.09$ ($P < 0.001$, uncorrected). In order to control for cumulating alpha errors, only clusters with a volume greater than 270 mm^3 (equivalent to 10 voxels) were considered. Blobs of activation were analyzed in more detail by extracting clusters around local maxima of activity. Local maxima were identified by peak activation within a search diameter of 6 voxels (18 mm) in any direction. For a separate analysis, Broca's area was defined as a primary volume of interest (VOI) for further investigation in order to define seed voxels for the reconstruction of fiber bundles. Within this VOI, local maxima were identified and beta values were compared across the 2 groups. A 2-sample *t*-test was conducted for identifying significant between-group differences.

Results

DTI: TBSS

We first explored differences in white matter FA between adults and children on the basis of TBSS (Smith et al. 2006). Direct comparison of FA between adults and children revealed significant differences in a number of regions including perisylvian white matter pathways. Particularly along the dorsal connection between frontal and temporal cortical regions (AF/SLF), a number of locations indicated differences in FA between groups (see Supplementary Figs 1 and 2, Supplementary Table 1). Underlying language-relevant cortical areas, group differences were observed in the white matter of the IFG and the middle and posterior part of the STG/STS (see Fig. 1) extending down to the border to MTG. In sum, these data argue for weaker axonal fiber connections and/or less myelination of language-relevant fibers in children compared with adults.

In order to identify affected fiber pathways more specifically, the language-relevant regions of significant FA differences between groups (IFG, STG/STS) were selected as seed regions of interest for a fiber tracking analysis. Results revealed that the 2 regions are directly interconnected via 2 independent connections, a dorsal pathway via the AF/SLF and a ventral pathway via the extreme capsule fiber system (ECFS) (Fig. 2). An additional analysis also

captured both connections, the AF/ SLF pathway and the ECFS pathway, when investigating the 2 groups separately.

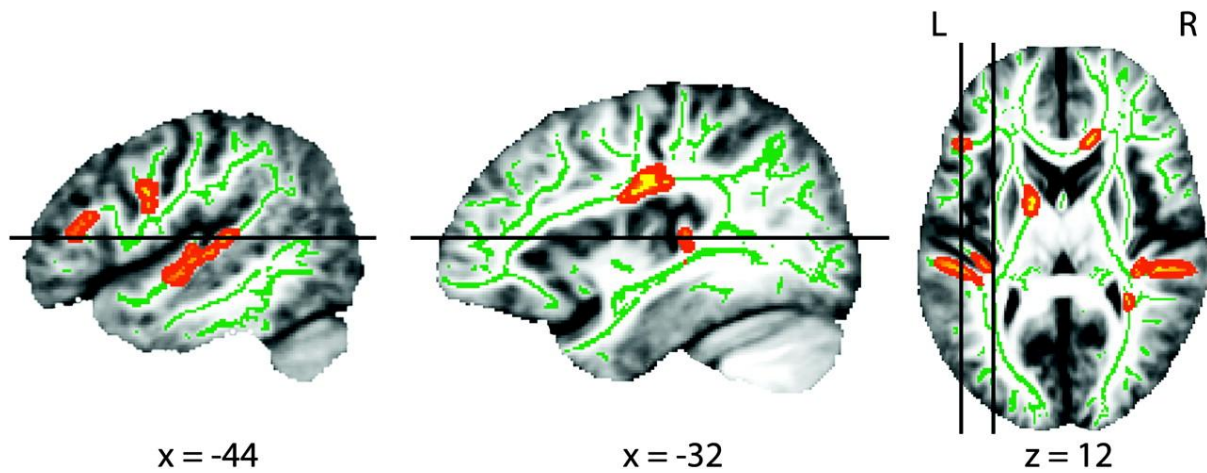


Figure 1: TBSS results for differences between adults and children. The figure represents a mean FA image with the white matter skeleton superimposed (in green). Regions of significant differences between groups are highlighted in red and filled into the local tract region of the mean FA image. They indicate lower FA in children compared with adults ($P < 0.05$, corrected) in the underlying white matter skeleton. Differences between groups are particularly found in Broca's (IFG) and Wernicke's language regions (STG/STS down to the MTG). The figure is displayed in 2 sagittal views and 1 axial view. Lines indicate location of the corresponding sections.

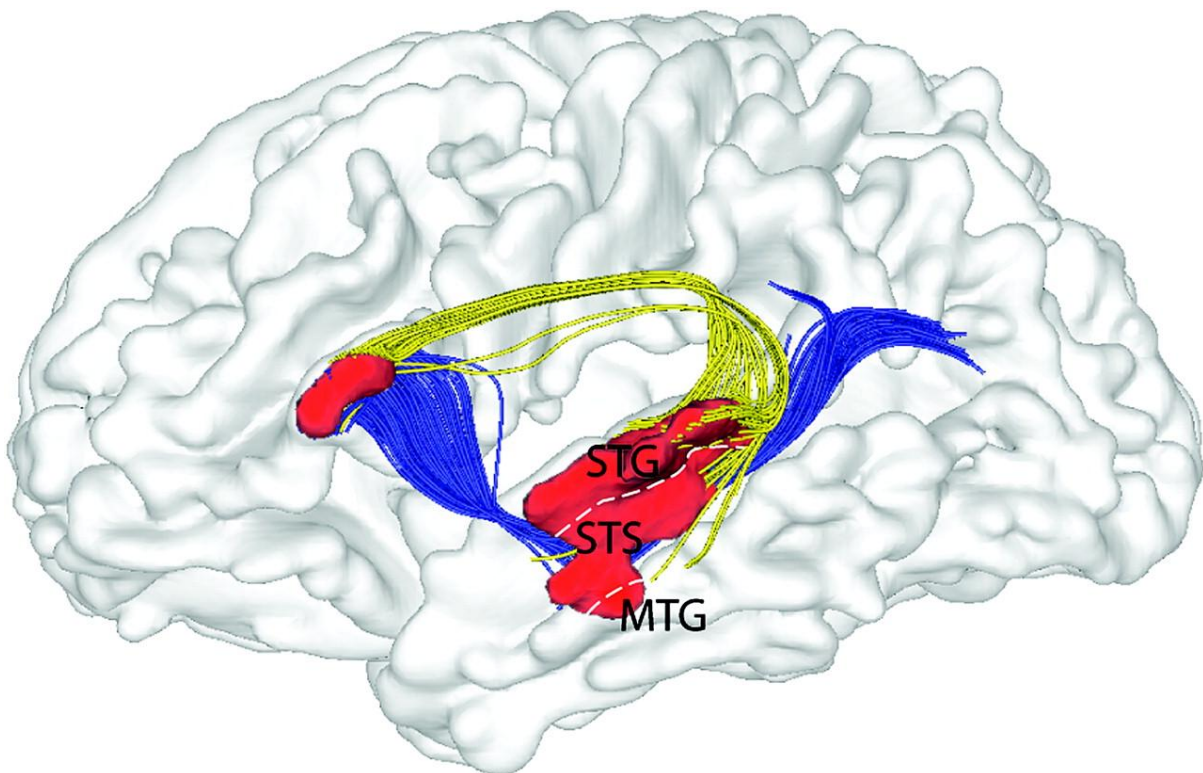


Figure 2: Fiber tracking of the DTI data averaged over both groups for the language relevant regions in IFG (frontal cluster) and STG/STS down to the MTG (temporal cluster) that showed

significant group differences in FA between adults and children in the white matter skeleton in TBSS. Fibers crossing both regions were regarded interconnecting bundles. The tracking reveals that these regions are connected via 2 separate white matter pathways, a dorsal connection via AF/SLF (in yellow) and a ventral connection via the ECFS (in blue). The pathways connecting the 2 significant regions (red) are shown onto the transparent smoothed white matter skeleton. The temporal cluster includes indications for the borders between STG, STS, and MTG.

fMRI Data

In a second step, these results of structural differences in white matter between adults and children were compared with functional activation patterns during language processing obtained from the same participants in a separate session. Behavioral task performance on a sentence comprehension task revealed no significant group differences but a trend in response correctness. Both groups showed high performance rates: adults 91.2% (SD 1.5), children 86.7% (SD 7.8), $t_{1,9} = 2.18$ ($P = 0.06$).

Functional data revealed activation in IFG and in STG/STS and also in further brain regions in both groups (see Fig. 3 and Supplementary Table 2A and 2B). IFG activation in adults in Broca's area was located in the dorsal portion of BA 44 with a maximum at $-53, 13, 15$ (Talairach coordinates, Talairach and Tournoux 1988, see Fig. 3C, upper row). In children, IFG activation included BA 44 and also the more anterior portion of Broca's area BA 45 with a maximum located at $-53, 22, 12$ in BA 45 (see Fig. 3A, upper row). Direct comparison between groups in BA 44 and in BA 45 demonstrated stronger activation in children than in adults in BA 45 at $-53, 22, 12$ ($t_{1,9} = 3.92$, $P < 0.001$), while in BA 44 no difference was found ($t_{1,9} = 1.01$, $P = 0.17$), that is, adults did not show stronger involvement than children in neither subregions of Broca's area (Fig. 3B).

Comparing DTI and fMRI Data

The involvement of Broca's area was further explored by DTI-based tractography seeded on the gray-to-white matter border that was located closest to the functional activation maxima in BA 44 and in BA 45 in the IFG. For the BA 44 activation maximum retrieved from adults at $-53, 13, 15$, the tractography seed point originated at $-48, 10, 15$. For the BA 45 activation maximum retrieved from children and the direct group comparison at $-53, 22, 12$, the seed point originated at $-42, 22, 10$. Tractography indicated a dorsal pathway from BA 44 via the AF/SLF connecting the activated area in the IFG with the STG/STS. For the BA 45 seeding,

tractography revealed a ventral pathway running from the IFG through the ECFS to the STG/STS (see Fig. 3, lower row).

Fiber tracking was cross-validated for both seeds. In children as well as in adults, tracking was seeded in both locations (BA 44 and BA 45) within Broca's area as described above. Results captured for both groups the dorsal pathway via the AF/SLF when tracking from the BA 44 seed and the ventral pathway via the ECFS when tracking from the BA 45 seed (see Supplementary Figure 3). Furthermore, tractography using a crossing fiber model (Behrens et al. 2007) revealed again the same dominant connections from BA 44 to AF/SLF and from BA 45 to the ECFS (see Supplementary Fig. 4). Hence, the fiber tracking reflects valid differences between adults and 7-year olds in the underlying connectivity of functionally recruited cortical areas in Broca's area (BA 44 and BA 45) that connect to STG/STS by separate pathways.

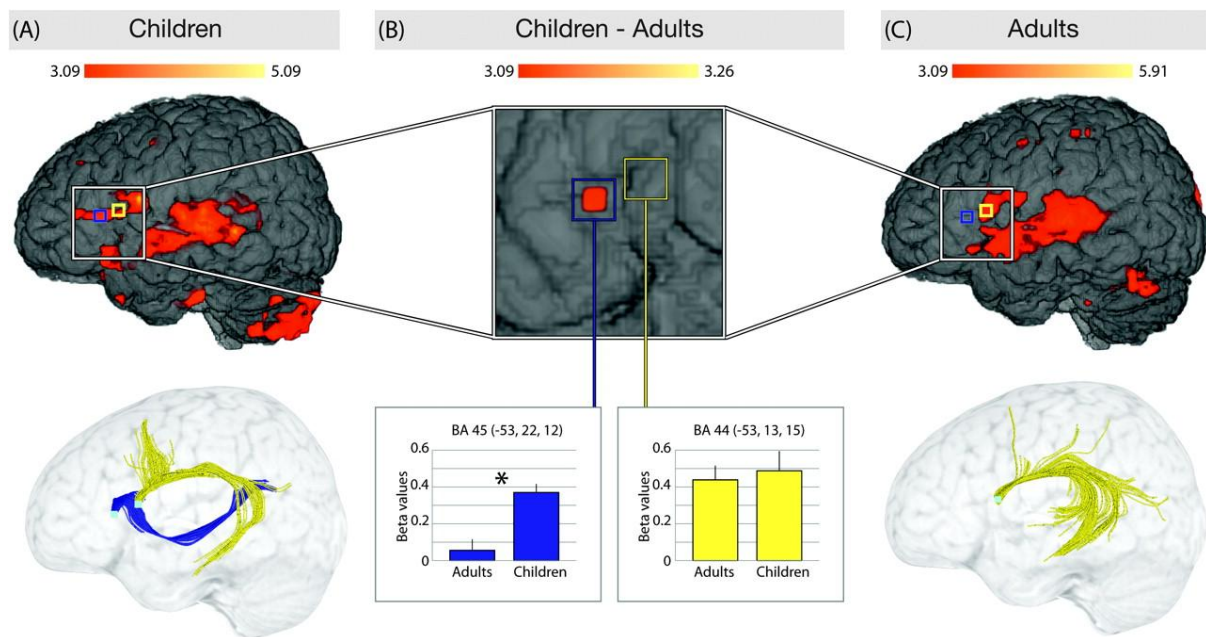


Figure 3: Functional activation during auditory language processing and corresponding tractography of fiber tract connections underlying activated regions in Broca's area. Upper row: activation z maps for children and adults during sentence comprehension versus resting baseline on a *T1* reference brain. Both groups activated areas in the perisylvian cortex in the IFG (Broca's area) and in the STG/STS (Wernicke's area). Second-level analysis for both groups resulted with parametric maps of z scores showing local maxima within the inferior frontal activation in BA 45 (-53, 22, 12, blue quadrant) for children (A) and in BA 44 (-53, 13, 15, yellow quadrant) for adults (C) (see also Supplementary Table 2A and 2B). Direct comparison (2-sample *t*-test) between groups in Broca's area (B) revealed that children involved BA 45 (-53, 22, 12) in addition to BA 44 activation, while adults did not show any stronger activation than children. These results indicate that children make use of both BA 44 and BA 45 in Broca's area, while adults recruit BA 44 only. Lower row: tractography in group averaged

DTI data based on functional activation in Broca's area with seed points (turquoise dots) in BA 45 (activation in children and direct group contrast, A,B) and BA 44 (activation in adults, C). Tracking result of activation in children captured the ECFS (in blue), a ventral connection between inferior frontal and superior temporal areas. Tracking result of activation in adults captured the AF/SLF (in yellow), a dorsal connection between these areas. In children (A), also the dorsal connection is displayed as a result of a tractography seeded in the adults' activation maximum. Functional data implicate that children make use of the ventral connection in addition to the dorsal connection that was revealed for adults. The size of the seed voxels was 3 x 3 x 3 mm.

Discussion

The present findings indicate that the brain's language network in children has not yet reached the same confined status as in adults. Rather, when processing sentence, 7-year-old children rely on alternative pathways connecting the cortical areas involved in language processing. Functional activation during auditory language comprehension demonstrates that adults employ the posterior portion of Broca's area (BA 44), that is, pars opercularis, while the main center of activation for children is found in the anterior portion of Broca's area (BA 45), that is, pars triangularis. Direct comparison of functional recruitment between adults and children reveals that BA 44 is activated in both adults and children, but that BA 45 of Broca's area is additionally activated in children. These results suggest that in children, pars opercularis alone does not suffice to accomplish the task of comprehending language. Rather, children appear to need supplementary cortical involvement within Broca's area. This is achieved by recruiting pars triangularis. Thus, it appears that children make use of their dorsal pathway to the temporal cortex, but since this is not sufficient due to its immaturity, they extend their frontotemporal connection network by making additional use of a ventral connection via the ECFS which already is more mature.

Previous DTI studies in adults reported convincing results by tracking white matter connections for coordinates as reported in existing functional studies on activation during language tasks (e.g., Glasser and Rilling 2008). Our methodology is supposedly even more accurate since we used functional and diffusion data from the identical group of participants. Tractography data of these centers of language processing in both groups reveal that the observed activation differences reflect the use of 2 separate pathways connecting the frontal and the temporal language areas. Children make additional use of BA 45, which connects via the ventral pathway along ECFS to the temporal cortex. Adults who, in contrast to children, primarily activate BA 44 rely on the dorsal pathway connecting inferior frontal and superior temporal language areas via the AF/SLF. In accordance with a previous study, this entire

dorsal pathway is labeled AF/SLF (Saur et al. 2008) since it is still not yet possible to reliably distinguish between single fibers that are contained in the fiber bundles of AF and of SLF that both originate in Broca's area, but which appear to terminate in different cortical regions (Catani et al. 2005; Rilling et al. 2008). It is known from monkey and human data that in this dorsal connection the SLF, probably with its subdivisions SLF II and SLF III, coexists with the AF (Makris et al. 2005; Petrides and Pandya 2006; Schmahmann et al. 2007; Frey et al. 2008). This dorsal pathway, which is dominant in human adults, appears to be functionally insufficient in children. The main reason for the supplementary use of the ventral pathway in the language network in young children might be the immature nature of the main connection via the AF/SLF. Direct comparison of fiber tract anisotropy of white matter fiber pathways supports this view. Children show lower values of FA in several white matter regions. For the perisylvian language-relevant region, these age-related differences show up particularly along the dorsal frontotemporal connection via the AF/SLF. Tractography results suggest that the dorsal connection to the temporal lobe includes direct connections to the STG/STS in both groups. However, Figure 3 (lower panel) seems to suggest between-group differences with much stronger terminations of the dorsal connection to the STG/STS in adults. Perhaps, it could be specifically a missing branch of the fiber tract that is least developed in children (cf. Supplementary Figure 3). A closer investigation of this finding, however, by tracking the 2 groups individually seeded from the whole FA difference clusters did not reveal a strong support for such connectivity differences between adults and children.

The ventral and the dorsal perisylvian pathways are expressed differently in humans and other primates. A ventral pathway along the ECFS has been described in the monkey brain (Romanski et al. 1999) and in humans (Frey et al. 2008; Hua et al. 2009; Makris and Pandya 2009). The dorsal pathway differs between human and nonhuman primates. In the monkey, the dorsal connection includes fibers from different subpathways of SLF and AF (Petrides and Pandya 2006; Schmahmann et al. 2007). For the initial parts of the dorsal connection, this appears to also be valid for the human brain (Makris et al. 2005; Frey et al. 2008). However, humans differ from nonhuman primates in that the former display stronger terminations in the posterior temporal cortex (Rilling et al. 2008).

It is interesting to note that the dorsal pathway in humans shows a very early asymmetry toward the language-dominant hemisphere already in infants (Dubois et al. 2009), while on the other hand it is among those white matter fiber connections that fully mature only very

late in human ontogeny (Giorgio et al. 2008). The present data argue for an immature AF/SLF in 7-year-old children compared with adults as measured by FA. It is particularly this dorsal fiber connection that shows age-related FA differences in several sections along its pathway. The structural distinction of the adult brain and the developing brain converges with functional activation differences in corresponding cortical language areas during sentence comprehension.

It has been shown that FA in language-related brain regions can predict performance in language-related tasks (Flores et al. 2009). Reduced FA, as observed in children, is probably a result of an immature axonal and myelination status (Paus 2010), which is likely to hamper the speed and accuracy of information transmission in these fasciculi (Jones 2004). Since impulse synchrony is important for neuronal association (Hebb 1949) and information processing (Gollisch and Meister 2008), timing and precision parameters become crucial for optimal behavioral and mental performance and also learning. Our results appear to correspond to results reporting correlations between FA and cognitive development (Schmithorst et al. 2005) and also to data on cognitive decline in aging that show additional recruitment of cortical areas and concurrent decline in white matter FA that seem to associate to loss of cognitive capacities (Persson et al. 2006). From a distributed network perspective on brain organization, more difficult information transfer between cortical regions based on immature white matter would lead to either smaller and more local networks in children (Fair et al. 2009) or, where this is not possible, to usage of additional network connections as we observed in our study. Activation differences between adults and children might reflect effects of task experience, attention, or strategy, even when behavioral outcomes are comparable. As proposed in a model on development of functional brain activation, experience might be a factor that interacts independently with both brain morphology and functional activation in relevant brain regions (Lu et al. 2009). Likewise, it is not possible to exclude differences in maturational or environmental individual histories between our samples of adults and children that could potentially contribute to the group differences as described above.

Language processing involves whole networks of brain areas (for reviews, see Vigneau et al. 2006; Hickok and Poeppel 2007; Doehrmann and Naumer 2008). The meta-analysis of Vigneau et al. (2006) indicates that the left IFG and the temporal cortex are the regions that support sentence processing. By focusing on activation peaks in Broca's area in our study, we

leave other areas also important for language comprehension undiscussed (for comprehensive data, see Supplementary Table 2A and 2B). Insofar, the activation clusters in BA 44 and BA 45 of Broca's area are not the only areas involved in sentence processing but certainly necessary parts of the network supporting the processing of human language.

Our findings raise the question of causal relations between structure and function. On the one hand, functional processing of language might be regarded as being dependent on existing structural prerequisites, hence arguing for a structure-to-function causal relationship. Causal influences of white matter structure on function can be concluded from studies on white matter effects on neurotransmitter functions (Roy et al. 2007) and from myelin-derived effects on axonal and synaptic growth (McKerracher and Winton 2002). Such interpretations of structure-to-function relations are, for example, entertained for the effects of structural corpus callosum connections on the perception of speech (Westerhausen et al. 2009). Viewed from this perspective, the present findings would argue for a deviating functional connection between Broca's and Wernicke's language regions in the developing brain. As long as the main fiber connection between these regions via the AF/ SLF is not yet fully mature, supplementary processing centers (in Broca's area BA 45) and communication pathways (via the ECFS) between the cortical areas involved in language comprehension are needed.

On the other hand, changes and adjustments in brain structure are subject to influence by functional use. This might also hold for processes of maturation and development, thus arguing for a function-to-structure causal relationship. From this perspective, the present findings would indicate that during development, increasing use of language-related brain circuits and ongoing experience shape the language network with the AF/SLF finally being the most important connection between Broca's and Wernicke's regions in the mature language processing system. Such effects of practice and experience on white matter brain structures during development were observed for nonhuman mammals (Markham and Greenough 2004) and also for human infants (Als et al. 2004). Myelination plasticity of white matter structures could therefore be regarded as providing a gliogenic mechanism of behavioral adaptation and learning that corresponds to the neuronal mechanism of synaptic plasticity. This viewpoint rests upon empirical findings supporting the assumption of environmental effects on white matter morphology (Fields 2008).

Final conclusions on structure--function causalities, however, are premature and need to be drawn with caution (Aslin and Schlaggar 2006). Rather, a synthesis of both points of view,

structure-to-function versus function-to-structure causal relations, might be the basis for learning and adaptation throughout the entire life cycle. During development and maturation, the brain concentrates processing capacities onto functional subsystems that are embodied in cortical regions and their corresponding white matter connections that are hence strengthened. These specialized regions and their connections form networks that in turn allow faster and more efficient information exchange. Beyond these considerations concerning the relationship of development and brain maturation, the present results also emphasize the brain's universal functional flexibility by defining alternative functional networks according to the structural options at its disposal.

Notes

The authors thank Marc Tittgemeyer for helpful comments on study design and Yves von Cramon, Roberto Cozatl, and Karsten Müller for helpful comments on a previous version of the manuscript.

References

- Achenbach TM. 1998. CBCL/4-18 Elternfragebogen über das Verhalten von Kindern und Jugendlichen [Child Behavior Checklist (CBCL/4-18)]. Cologne (Germany): Arbeitsgruppe Kinder- Jugend- und Familiendiagnostik (KJFD). (Original work published 1991).
- Als H, Duffy FH, McAnulty GB, Rivkin MJ, Vajapeyam S, Mulkern RV, Warfield SK, Huppi PS, Butler SC, Conneman N, et al. 2004. Early experience alters brain function and structure. *Pediatrics*. 113:846--857.
- Anwander A, Tittgemeyer M, von Cramon DY, Friederici AD, Knösche TR. 2007. Connectivity-based parcellation of Broca's area. *Cereb Cortex*. 17:816--825.
- Aslin RN, Schlaggar BL. 2006. Is myelination the precipitating neural event for language development in infants and toddlers? *Neurology*. 66:304--305.
- Barnea-Goraly N, Menon V, Eckert M, Tamm L, Bammer R, Karchemskiy A, Dant CC, Reiss AL. 2005. White matter development during childhood and adolescence: a cross-sectional diffusion tensor imaging study. *Cereb Cortex*. 15:1848--1854.
- Behrens TEJ, Berg HJ, Jbabdi S, Rushworth MFS, Woolrich MW. 2007. Probabilistic diffusion tractography with multiple fibre orientations: what can we gain? *Neuroimage*. 34:144--155.
- Bornkessel I, Zysset S, Friederici AD, von Cramon DY, Schlesewsky M. 2005. Who did what to whom? The neural basis of argument hierarchies during language comprehension. *Neuroimage*. 26:221--233.

- Brauer J, Friederici AD. 2007. Functional neural networks of semantic and syntactic processes in the developing brain. *J Cogn Neurosci.* 19:1609--1623.
- Brauer J, Neumann J, Friederici AD. 2008. Temporal dynamics of perisylvian activation during language processing in children and adults. *Neuroimage.* 41:1485--1493.
- Burock MA, Buckner RL, Woldorff MG, Rosen BR, Dale AM. 1998. Randomized event-related experimental designs allow for extremely rapid presentation rates using functional MRI. *Neuroreport.* 9:3735--3739.
- Casey BJ, Tottenham N, Liston C, Durston S. 2005. Imaging the developing brain: what have we learned about cognitive development? *Trends Cogn Sci.* 9:104--110.
- Catani M, Jones DK, Ffytche DH. 2005. Perisylvian language networks of the human brain. *Ann Neurol.* 57:8--16.
- Cohen Kadosh K, Johnson MH. 2007. Developing a cortex specialized for face perception. *Trends Cogn Sci.* 11:367--369.
- Constable RT, Pugh KR, Berroya E, Mencl WE, Westerveld M, Ni WJ, Shankweiler D. 2004. Sentence complexity and input modality effects in sentence comprehension: an fMRI study. *Neuroimage.* 22:11--21.
- Dittmar M, Abbot-Smith K, Lieven E, Tomasello M. 2008. German children's comprehension of word order and case marking in causative sentences. *Child Dev.* 79:1152--1167.
- Doehrmann O, Naumer MJ. 2008. Semantics and the multisensory brain: how meaning modulates processes of audio-visual integration. *Brain Res.* 1242:136--150.
- Dubois J, Dehaene-Lambertz G, Perrin M, Mangin JF, Cointepas Y, Duchesnay E, LeBihan D, Hertz-Pannier L. 2008. Asynchrony of the early maturation of white matter bundles in healthy infants: quantitative landmarks revealed noninvasively by diffusion tensor imaging. *Hum Brain Mapp.* 29:14--27.
- Dubois J, Hertz-Pannier L, Cachia A, Mangin JF, Le Bihan D, Dehaene-Lambertz G. 2009. Structural asymmetries in the infant language and sensori-motor networks. *Cereb Cortex.* 19:414--423.
- Fair DA, Cohen AL, Power JD, Dosenbach NUF, Church JA, Miezin FM, Schlaggar BL, Petersen SE. 2009. Functional brain networks develop from a "local to distributed" organization. *PLoS Comput Biol.* 5:e1000381.
- Fields RD. 2008. White matter in learning, cognition and psychiatric disorders. *Trends Neurosci.* 31:361--370.
- Fillard P, Pennec X, Arsigny V, Ayache N. 2007. Clinical DT-MRI estimation, smoothing, and fiber tracking with log-euclidean metrics. *IEEE Trans Med Imaging.* 26:1472--1482.
- Flöel A, de Vries MH, Scholz J, Breitenstein C, Johansen-Berg H. 2009. White matter integrity in the vicinity of Broca's area predicts grammar learning success. *Neuroimage.* 47:1974--1981.

- Frey S, Campbell JSW, Pike GB, Petrides M. 2008. Dissociating the human language pathways with high angular resolution diffusion fiber tractography. *J Neurosci.* 28:11435--11444.
- Friederici AD. 2002. Towards a neural basis of auditory sentence processing. *Trends Cogn Sci.* 6:78--84.
- Friederici AD. 2009a. Allocating functions to fiber tracts: facing its indirectness. *Trends Cogn Sci.* 13:370--371.
- Friederici AD. 2009b. Pathways to language: fiber tracts in the human brain. *Trends Cogn Sci.* 13:175--181.
- Friederici AD, Bahlmann J, Heim S, Schubotz RI, Anwander A. 2006. The brain differentiates human and non-human grammars: functional localization and structural connectivity. *Proc Natl Acad Sci U S A.* 103:2458--2463.
- Friederici AD, Fiebach CJ, Schlesewsky M, Bornkessel ID, von Cramon DY. 2006. Processing linguistic complexity and grammaticality in the left frontal cortex. *Cereb Cortex.* 17:1709--1717.
- Friston KJ, Fletcher P, Josephs O, Holmes A, Rugg MD, Turner R. 1998. Event-related fMRI: characterizing differential responses. *Neuroimage.* 7:30--40.
- Gaillard WD, Hertz-Pannier L, Mott SH, Barnett AS, LeBihan D, Theodore WH. 2000. Functional anatomy of cognitive development - fMRI of verbal fluency in children and adults. *Neurology.* 54:180--185.
- Ghazanfar AA. 2008. Language evolution: neural differences that make a difference. *Nat Neurosci.* 11:382--384.
- Giorgio A, Watkins KE, Douaud G, James AC, James S, De Stefano N, Matthews PM, Smith SM, Johansen-Berg H. 2008. Changes in white matter microstructure during adolescence. *Neuroimage.* 39:52--61.
- Glasser MF, Rilling JK. 2008. DTI tractography of the human brain's language pathways. *Cereb Cortex.* 18:2471--2482.
- Gollisch T, Meister M. 2008. Rapid neural coding in the retina with relative spike latencies. *Science.* 319:1108--1111.
- Grimm H, Schoeler H. 1991. *Heidelberger Sprachentwicklungstest (HSET)*. 2nd ed. Göttingen (Germany): Hogrefe.
- Hahne A, Eckstein K, Friederici AD. 2004. Brain signatures of syntactic and semantic processes during children's language development. *J Cogn Neurosci.* 16:1302--1318.
- Hashimoto R, Sakai KL. 2002. Specialization in the left prefrontal cortex for sentence comprehension. *Neuron.* 35:589--597.
- Hebb DO. 1949. *The organization of behavior*. New York: John Wiley xix + 335 pp.
- Hickok G, Poeppel D. 2007. Opinion—the cortical organization of speech processing. *Nat Rev Neurosci.* 8:393--402.

- Hua K, Oishi K, Zhang J, Wakana S, Yoshioka T, Zhang W, Akhter KD, Li X, Huang H, Jiang H, et al. 2009. Mapping of functional areas in the human cortex based on connectivity through association fibers. *Cereb Cortex*. 19:1889--1895.
- Jenkinson M, Bannister P, Brady M, Smith S. 2002. Improved optimization for the robust and accurate linear registration and motion correction of brain images. *Neuroimage*. 17:825--841.
- Jones DK, Symms MR, Cercignani M, Howard RJ. 2005. The effect of filter size on VBM analyses of DT-MRI data. *Neuroimage*. 26:546--554.
- Jones R. 2004. Myelin. made to measure. *Nat Rev Neurosci*. 5:343.
- Josephs O, Turner R, Friston K. 1997. Event-related fMRI. *Hum Brain Mapp*. 5:243--248.
- Kaufman AS, Kaufman NL. 1994. Kaufman assessment battery for children (K-ABC). [German version: Melchers P, Preuss U.] 2nd ed. Lisse, Netherlands: Swets & Zeitlinger BV.
- Lazar M, Weinstein DM, Tsuruda JS, Hasan KM, Arfanakis K, Meyerand ME, Badie B, Rowley HA, Haughton V, Field A, et al. 2003. White matter tractography using diffusion tensor deflection. *Hum Brain Mapp*. 18:306--321.
- Lebel C, Walker L, Leemans A, Phillips L, Beaulieu C. 2008. Microstructural maturation of the human brain from childhood to adulthood. *Neuroimage*. 40:1044--1055.
- Lenroot RK, Giedd JN. 2006. Brain development in children and adolescents: insights from anatomical magnetic resonance imaging. *Neurosci Biobehav Rev*. 30:718--729.
- Lohmann G, Müller K, Bosch V, Mentzel H, Hessler S, Chen L, Zysset S, von Cramon DY. 2001. LIPSIA - a new software system for the evaluation of functional magnetic resonance images of the human brain. *Comput Med Imaging Graph*. 25:449--457.
- Lu LH, Dapretto M, O'Hare ED, Kan E, McCourt ST, Thompson PM, Toga AW, Bookheimer SY, Sowell ER. 2009. Relationships between brain activation and brain structure in normally developing children. *Cereb Cortex*. 19:2595--2604.
- Makris N, Kennedy DN, McInerney S, Sorensen AG, Wang R, Caviness VS, Pandya DN. 2005. Segmentation of subcomponents within the superior longitudinal fascicle in humans: a quantitative, in vivo, DT-MRI study. *Cereb Cortex*. 15:854--869.
- Makris N, Pandya D. 2009. The extreme capsule in humans and rethinking of the language circuitry. *Brain Struct Funct*. 213:343--358.
- Markham JA, Greenough WT. 2004. Experience-driven brain plasticity: beyond the synapse. *Neuron Glia Biol*. 1:351--363.
- McKerracher L, Winton MJ. 2002. Nogo on the go. *Neuron*. 36:345--348.
- Mukherjee P, Miller JH, Shimony JS, Conturo TE, Lee BCP, Almlil CR, McKinstry RC. 2001. Normal brain maturation during childhood: developmental trends characterized with diffusion-tensor MR imaging. *Radiology*. 221:349--358.

- Norris DG. 2000. Reduced power multislice MDEFT imaging. *J Magn Reson Imaging*. 11:445--451.
- Paus T. 2010. Growth of white matter in the adolescent brain: myelin or axon? *Brain Cogn*. 72:26--35.
- Persson J, Nyberg L, Lind J, Larsson A, Nilsson LG, Ingvar M, Buckner RL. 2006. Structure-function correlates of cognitive decline in aging. *Cereb Cortex*. 16:907--915.
- Petkov CI, Logothetis NK, Obleser J. 2009. Where are the human speech and voice regions and do other animals have anything like them? *Neuroscientist*. 15:419--429.
- Petrides M, Pandya DN. 2006. Efferent association pathways originating in the caudal prefrontal cortex in the macaque monkey. *J Comp Neurol*. 498:227--251.
- Reese TG, Heid O, Weisskoff RM, Wedeen VJ. 2003. Reduction of eddy-current-induced distortion in diffusion MRI using a twice-refocused spin echo. *Magn Reson Med*. 49:177--182.
- Rilling JK, Glasser MF, Preuss TM, Ma XY, Zhao TJ, Hu XP, Behrens TEJ. 2008. The evolution of the arcuate fasciculus revealed with comparative DTI. *Nat Neurosci*. 11:426--428.
- Rivera SM, Reiss AL, Eckert MA, Menon V. 2005. Developmental changes in mental arithmetic: evidence for increased functional specialization in the left inferior parietal cortex. *Cereb Cortex*. 15:1779--1790.
- Rogalsky C, Matchin W. 2008. Hickok G. 2008. Broca's area, sentence comprehension, and working memory: an fMRI study. *Front Hum Neurosci*. 2:14.
- Romanski LM, Tian B, Fritz J, Mishkin M, Goldman-Rakic PS, Rauschecker JP. 1999. Dual streams of auditory afferents target multiple domains in the primate prefrontal cortex. *Nat Neurosci*. 2:1131--1136.
- Roy K, Murtie JC, El Khodort BF, Edgar N, Sardi SP, Hooks BM, Benoit-Marand M, Chen CF, Moore H, O'Donnell P, et al. 2007. Loss of erbB signaling in oligodendrocytes alters myelin and dopaminergic function, a potential mechanism for neuropsychiatric disorders. *Proc Natl Acad Sci U S A*. 104:8131--8136.
- Saur D, Kreher BW, Schnell S, Kämmerer D, Kellmeyer P, Vry M-S, Umarova R, Musso M, Glauche V, Abel S, et al. 2008. Ventral and dorsal pathways for language. *Proc Natl Acad Sci U S A*. 105:18035--18040.
- Schlaggar BL, Church JA. 2009. Functional neuroimaging insights into the development of skilled reading. *Curr Dir Psychol Sci*. 18:21--26.
- Schmahmann JD, Pandya DN, Wang R, Dai G, D'Arceuil HE, de Crespigny AJ, Wedeen VJ. 2007. Association fibre pathways of the brain: parallel observations from diffusion spectrum imaging and autoradiography. *Brain*. 130:630--653.

- Schmithorst VJ, Wilke M, Dardzinski BJ, Holland SK. 2005. Cognitive functions correlate with white matter architecture in a normal pediatric population: a diffusion tensor MRI study. *Hum Brain Mapp.* 26:139--147.
- Smith SM, Jenkinson M, Johansen-Berg H, Rueckert D, Nichols TE, Mackay CE, Watkins KE, Ciccarelli O, Cader MZ, Matthews PM, et al. 2006. Tract-based spatial statistics: voxelwise analysis of multisubject diffusion data. *Neuroimage.* 31:1487--1505.
- Smith SM, Jenkinson M, Woolrich MW, Beckmann CF, Behrens TEJ, Johansen-Berg H, Bannister PR, De Luca M, Drobnjak I, Flitney DE, et al. 2004. Advances in functional and structural MR image analysis and implementation as FSL. *Neuroimage.* 23:S208--S219.
- Snijders TM, Vosse T, Kempen G, Van Berkum JJA, Petersson KM, Hagoort P. 2009. Retrieval and unification of syntactic structure in sentence comprehension: an fMRI study using word-category ambiguity. *Cereb Cortex.* 19:1493--1503.
- Stromswold K. 1996. Genes, specificity, and the lexical/functional distinction in language acquisition. *Behav Brain Sci.* 19:648ff.
- Talairach J, Tournoux P. 1988. Co-planar stereotactic atlas of the human brain. New York: Thieme.
- Tyler LK, Marslen-Wilson W. 2008. Fronto-temporal brain systems supporting spoken language comprehension. *Philos Trans R Soc Lond B Biol Sci.* 363:1037--1054.
- Ugurbil K, Garwood M, Ellermann J, Hendrich K, Hinke R, Hu XP, Kim SG, Menon R, Merkle H, Ogawa S, et al. 1993. Imaging at high magnetic fields—initial experiences at 4 T. *Magn Reson Q.* 9:259--277.
- Vigneau M, Beaucousin V, Herve' PY, Duffau H, Crivello F, Houdé O, Mazoyer B, Tzourio-Mazoyer N. 2006. Meta-analyzing left hemispherelanguage areas: phonology, semantics, and sentence processing. *Neuroimage.* 30:1414--1432.
- Weiller C, Musso M, Rijntjes M, Saur D. 2009. Please don't underestimate the ventral pathway in language. *Trends Cogn Sci.* 13:369--370.
- Westerhausen R, Gruner R, Specht K, Hugdahl K. 2009. Functional relevance of interindividual differences in temporal lobe callosal pathways: a DTI tractography study. *Cereb Cortex.* 19:1322--1329.
- Wilke M, Lidzba K, Kra'geloh-Mann I. 2009. Combined functional and causal connectivity analyses of language networks in children: a feasibility study. *Brain Lang.* 108:22--29.
- Worsley KJ, Liao CH, Aston J, Petre V, Duncan GH, Morales F, Evans AC. 2002. A general statistical analysis for fMRI data. *Neuroimage.* 15:1--15.

Supplementary Material:

Neuroanatomical Prerequisites for Language Functions in the Maturing Brain

Jens Brauer, Alfred Anwander, & Angela D. Friederici

Max Planck Institute for Human Cognitive and Brain Sciences

Leipzig, Germany

Supplementary material includes:

supplementary text, supplementary tables (2), supplementary figures (4)

Supplementary Methods

For a careful approach of comparing child and adult brain imaging data, we tested the option of a joint image normalization for children and adults on a common standard space in order to conduct direct statistical comparison. White matter group differences between children and adults were compared statistically for FA image deformation on a joint normalization including both groups. Deformational vector fields were obtained for a nonlinear normalization on a common standard space. The target image for this procedure was selected on the basis of mutual alignment of every FA image on every other to identify the most representative FA image for the whole sample according to Smith et al. (2006). Values of image distortions for alignment were extracted and for each voxel in each individual FA image and compared on the basis of a repeated measures 2 (Group) \times 3 (Dimension) GLM. Results revealed no main effect for Group [$F(1, 17) < 1$], nor Dimension [$F(2, 34) = 1.1, p = 0.33$], nor a significant interaction [$F(2, 34) < 1$]. Thus, there were no differences between groups in the amount of image distortion for nonlinear normalization on a common source model. These results support the conclusion of low between-subject variance regarding the white matter tract alignment, even between children and adults. Accordingly, both groups were normalized on a common standard space.

Nonlinear normalization was also compared for whole brain T1 images. The same individual data as for the FA images alignment which was closest to the entire group mean served as source image for the normalization of T1 images. Values of image distortion were extracted for each voxel and compared statistically on basis of a repeated measures 2 (Group) \times 3 (Dimension) GLM. There was no main effect for Group [$F(1, 17) < 1$] and also main effect for Dimension [$F(2, 34) < 1$], nor a significant interaction [$F(2, 34) < 1$]. Thus, also for cortical normalization, the brains of children at this age are comparable to adult brains and both groups could be normalized on a common brain. This result is in accordance with previous conclusions about the possibility of a direct comparison between adults and children at age 7 on a common stereotactic space (Burgund ED et al. 2002).

Children are more likely to produce head motion during MR scanning (Yuan W et al. 2009). In order to avoid artifacts in the results, we were cautious with possible effects of motion. We controlled for motion in the functional MR data by (i) inspecting each single dataset for movement artefacts, (ii) applying a motion correction algorithm up to 3 mm (1 voxel) or otherwise (iii) excluding children with too much movement, and (iv) including motion parameters into the GLM. The diffusion weighted images were controlled in a similar way. The data was controlled for motion artefacts and corrected for subject motion using interleaved non diffusion weighted images (after each block of 10 diffusion weightings). The motion correction parameters were interpolated to all intermediate images and the diffusion directions were corrected for subject rotation before averaging three repetitions. In one subject, the rotation was bigger than 5° . To avoid angular blurring of the data from the three repeated acquisition of the same diffusion direction affected by the subject rotation, the three acquisitions were not averaged in this subject, but the tensor was computed from all individual measurements, which is more robust in this case. The quality of the motion correction was controlled by checking motion-sensitive anatomical landmarks in the DTI image like the anterior commissure. Moreover, motion estimates were statistically compared between groups in a repeated measurements ANOVA. For functional data, there was an interaction between group and the dimension of dislocation, $F(1,18) = 9.20$, $P < 0.01$, indicating that translations and rotations contributed differently to overall movement between groups. However, there was no group main effect in movement $F(1,18) < 1$. For diffusion data, there was again no group main effect, $F(1,18) < 1$, nor an interaction, $F(1,18) < 1$. Hence, the contribution of motion differences between groups can be neglected to contribute to observed group differences in either functional or diffusion data.

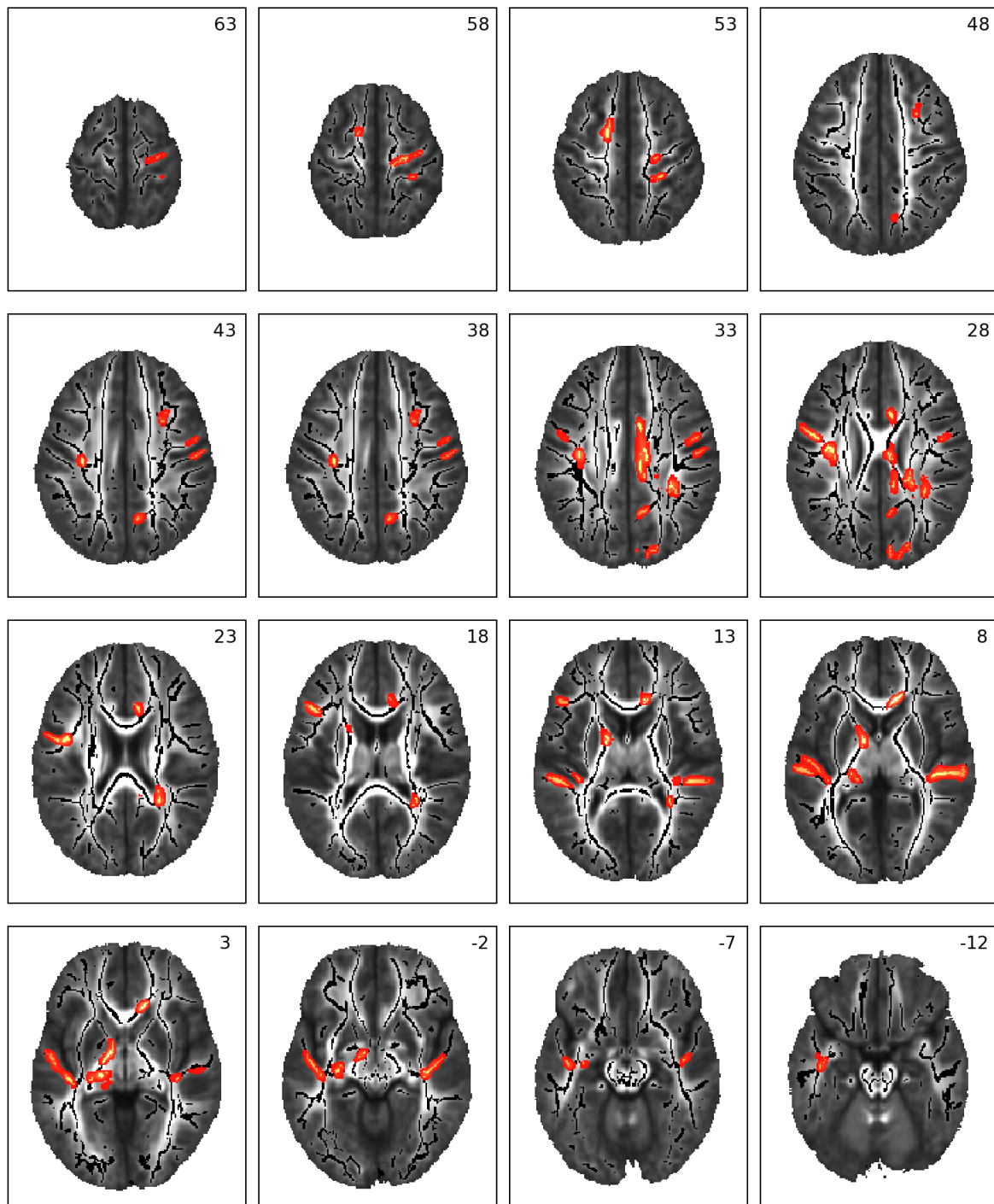
Supplementary Figure 1: Tract-based spatial statistics (TBSS) comparing cerebral white matter tracts between adults and children. Images display axial slicing through the mean fractional anisotropy (FA) image. Each slice is indexed by the Talairach z -coordinate. The white matter skeleton is superimposed on the images (in black). Regions in red indicate significant FA differences between adults and children ($p < .05$, corrected) and are filled into the local tract region. Skeletonization was processed for whole cerebral white matter (without thalamus and cerebellum). See Supplementary Figure 2 for a comprehensive list of regions with significant FA differences between groups.

Supplementary Figure 2: TBSS results for the adults vs. children contrast in FA. The figure lists regions with significant differences in FA between adults and children ($p < .05$, corrected). See Supplementary Table 2 for location and cluster size information for each region. Abbreviations: ACR = anterior corona radiata, CC = corpus callosum, CST = corticospinal tract, IC = internal capsule, IFG = inferior frontal gyrus, ILF = inferior longitudinal fasciculus, L = left, R = right, SLF = superior longitudinal fasciculus, SMA = supplementary motor area, STG = superior temporal gyrus, PCG = precentral gyrus, PCR = posterior corona radiate.

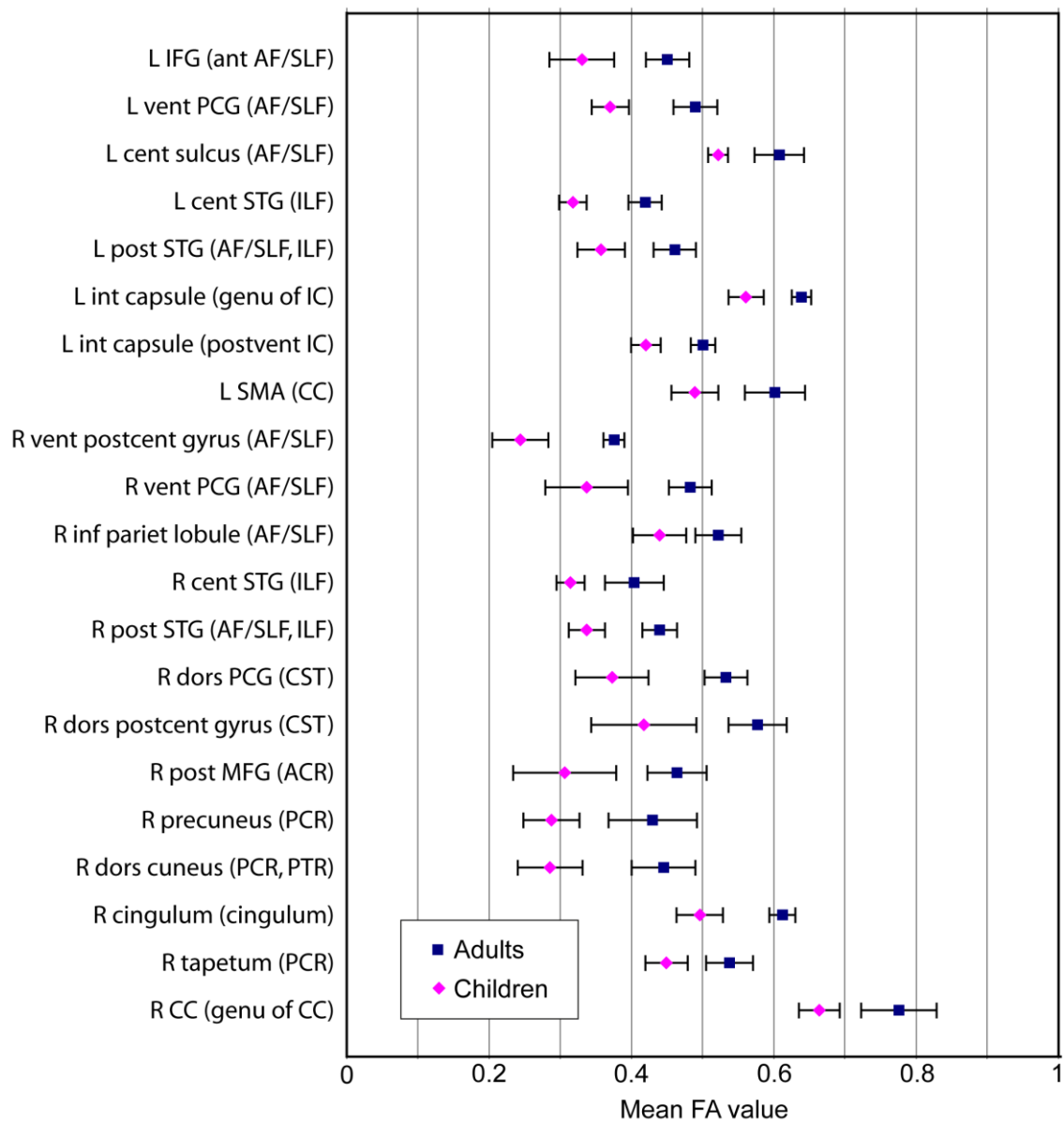
Supplementary Figure 3: Fiber tracking in both groups based on the two distinct activation maxima as observed for adults and children. The data show that white matter connections are similar for children and adults. Also children show the dorsal connection via the AF/SLF when seeding for the adults' maximum activation center. Likewise, also adults show the ventral connection via the ECFS when seeding for the children's maximum activation center. Thus, functional activation differences between adults and children are indeed related to alternative connections between IFG and STG/STS in both groups. The size of the seed voxels was 3 x 3 x 3 mm.

Supplementary Figure 4: Probabilistic tractography using a crossing fiber model for projections from BA 45 (left panel) and BA 44 (right panel). Images display sagittal (upper row) and coronal slices (lower row) of a T1 weighted anatomical image in several slices. Each slice is indexed by the Talairach coordinate. The group probability fiber connection map for BA 44 and BA 45 is

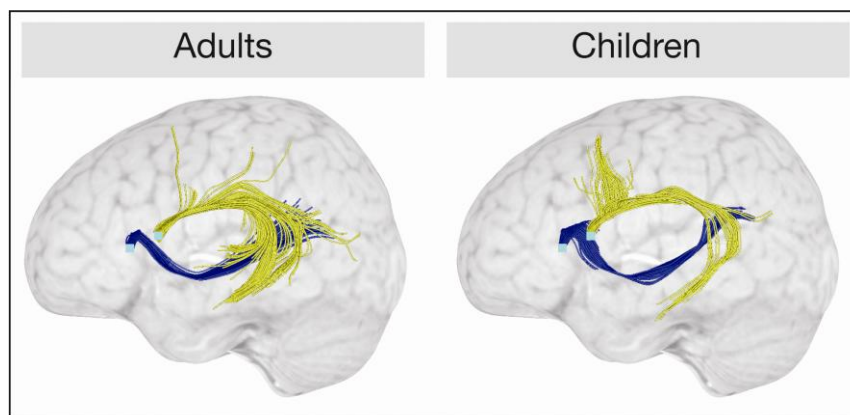
superimposed on the images. The color indicates the number of subjects with a pathway at that voxel. These maps were generated from individual probabilistic tractograms (10,000 tracts) and binarized with a minimum of 10 tracts per voxel. The binary tractograms were aligned by nonlinear normalization using the corresponding FA images and combined to a group probability map. The results agree with the single tensor model findings by revealing dominant connections from BA 44 to AF/SLF and from BA 45 to the ECFS. In addition, BA 44 connects to the rostral supplementary motor area (pre SMA), and BA 45 connects to the Thalamus via the anterior thalamic radiation (ATR).



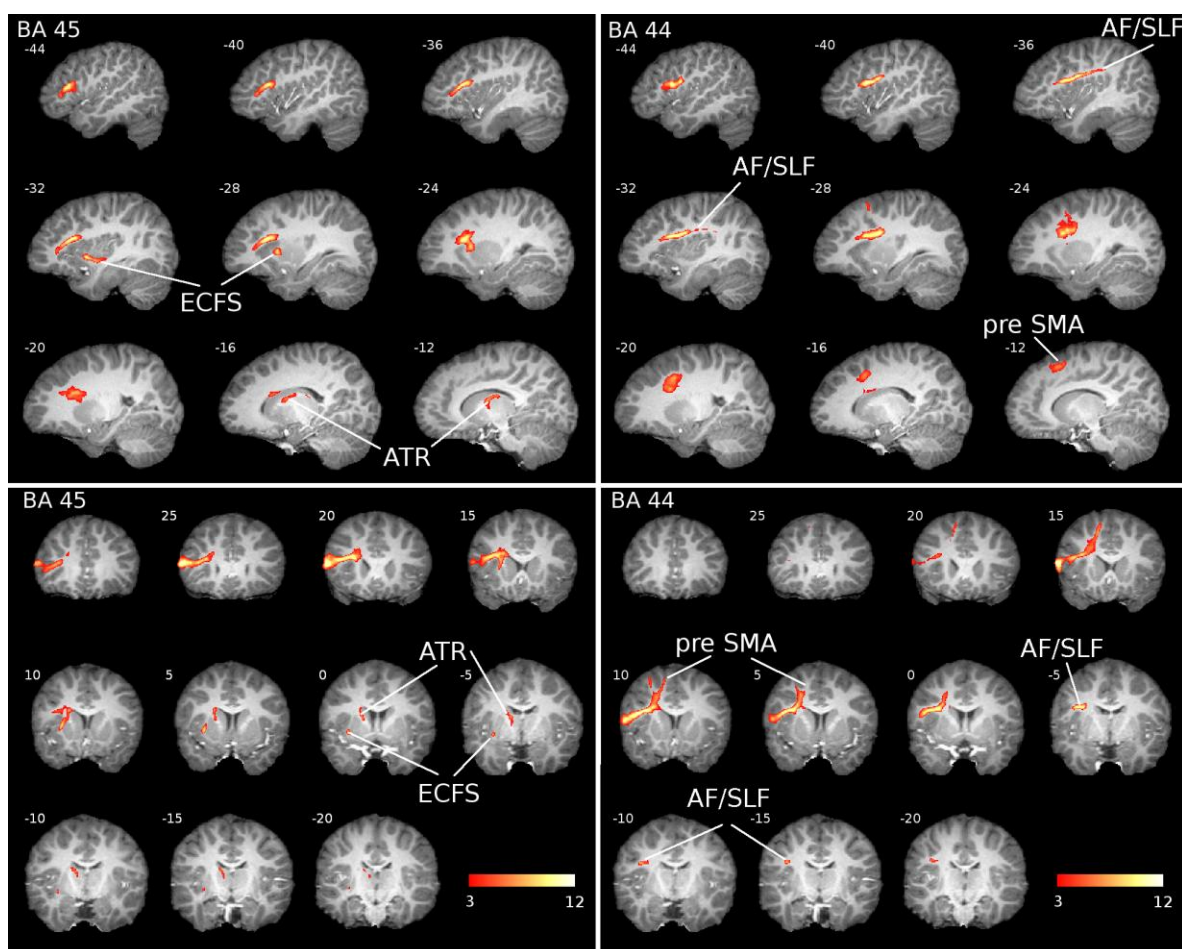
Supplementary Figure 1



Supplementary Figure 2



Supplementary Figure 3



Supplementary Figure 4

Supplementary Table 1: The table lists regions of significant white matter differences ($P < .05$, corrected) in FA between adults and children including location (Talairach coordinates) and cluster size (in mm^3). All regions indicated lower FA values in children than in adults (cf. Supplementary Figure 1). There was no region with higher FA in children than in adults. Abbreviations: ACR = anterior corona radiata, CC = corpus callosum, CST = corticospinal tract, IC = internal capsule, IFG = inferior frontal gyrus, ILF = inferior longitudinal fasciculus, GM = gray matter, L = left, R = right, SLF = superior longitudinal fasciculus, SMA = supplementary motor area, STG = superior temporal gyrus, PCG = precentral gyrus, PCR = posterior corona radiate.

Region	Location (x y z)			Size in mm^3
L IFG (ant AF/SLF)	-45	22	17	96
L vent PCG (AF/SLF)	-45	-1	27	194
L cent sulcus (AF/SLF)	-32	-18	35	144
L cent STG (ILF)	-43	-18	1	497
L post STG (AF/SLF, ILF)	-49	-28	12	82
L int capsule (genu of IC)	-13	-3	6	204
L int capsule (postvent IC)	-15	-28	6	165
L SMA (CC)	-14	-2	54	91
R vent postcent gyrus (AF/SLF)	47	-13	35	78
R vent PCG (AF/SLF)	44	-4	34	83
R inf pariet lobule (AF/SLF)	29	-35	32	86
R cent STG (ILF)	38	-10	-6	156
R post STG (AF/SLF, ILF)	46	-25	9	372
R dors PCG (CST)	18	-21	59	114
R dors postcent gyrus (CST)	24	-33	60	96
R post MFG (ACR)	25	13	43	85
R precuneus (PCR)	8	-56	36	136
R dors cuneus (PCR, PTR)	11	-82	29	100
R cingulum (cingulum)	8	-7	31	363
R tapetum (PCR)	22	-45	25	174
R CC (genu of CC)	11	25	2	138

Supplementary Table 2A: Gray matter brain regions reliably activated in adults listed with Brodmann areas (BAs), location in Talairach coordinates (x, y, z), and maximum z-value for the main contrast of sentence comprehension against resting baseline (null events).

Region	Left Hemisphere			Right Hemisphere		
	BA	Location	Z-max	BA	Location	Z-max
Inferior Frontal Gyrus	44	-53 13 15	4.25			
Inferior Frontal Gyrus	47	-47 22 -3	4.29			
Frontal Operculum	47	-32 25 6	5.48			
Frontal Operculum		-23 16 18	4.29		31 16 3	5.14
Sup Temp Gyrus	41	-56 -20 6	6.06	41	49 -26 9	6.02
Sup Temp Gyrus				38	52 4 -6	4.75
Precentral Gyrus	6	-50 -2 48	3.76	6	25 -14 57	4.04
Precentral Gyrus				6	43 -2 42	3.62
Postcentral Gyrus	2	-53 -23 33	3.98			
Sup Front Gyrus	6	-2 13 51	5.01	10	28 46 24	3.92
Med Front Gyrus				6	10 -5 54	3.75
Insula	13	-32 -35 24	5.00			
Inf Pariet Cortex	40	-53 -35 54	3.64			
Cuneus	19	-2 -95 24	4.30			
Cuneus	17	-11 -77 9	4.18			
Precuneus	7	-5 -74 54	4.14	7	7 -83 48	4.43
Cingulate Cortex	30	-23 -62 9	4.31			
Cingulate Cortex	32	-8 19 36	4.99	32	10 19 33	4.41
Basal Ganglia		-20 -8 6	4.25		25 -11 -6	4.59
Basal Ganglia					7 10 0	4.19
Fusiform Gyrus	37	-38 -53 -9	4.12			
Clastrum		-35 -8 -9	4.62		28 1 21	4.84
Cerebellum		-11 -44 -21	4.52		13 -65 -15	4.77
Cerebellum		-38 -62 -18	5.13			
Cerebellum		-11 -68 -24	4.08			

Supplementary Table 2B: Gray matter brain regions reliably activated in children listed with Brodmann areas (BAs), location in Talairach coordinates (x, y, z), and maximum z-value for the main contrast of sentence comprehension against resting baseline (null events).

Region	Left Hemisphere			Right Hemisphere		
	BA	Location	Z-max	BA	Location	Z-max
Inferior frontal gyrus	45	-53 22 12	3.99	44	58 13 15	4.56
Inferior frontal gyrus	47	-50 22 -9	4.17	47	22 10 -21	4.20
Frontal Operculum		-23 19 -6	4.02		31 16 0	4.55
Sup Front Gyrus	10	-14 61 24	3.49			
Sup Front Gyrus	6	-11 13 48	4.59			
Sup Temp Gyrus	38	-32 13 -21	3.69	38	46 19 -12	4.39
Sup Temp Gyrus				22	46 -23 0	5.13
Mid Temp Gyrus	22	-62 -41 6	4.97			
Inf Temp Gyrus				20	49 -2 -33	4.39
Mid Front Gyrus	9	-38 10 24	3.83	46	55 34 15	4.18
Precentral Gyrus	6	-59 4 21	4.79			
Precentral Gyrus	6	-44 -5 48	4.12	6	34 -8 51	3.94
Postcentral Gyrus	3	-38 -20 45	3.84	3	34 -23 45	4.41
Paracentral Cortex	31	-5 -17 48	3.85			
Sup Pariet Cortex	7	-29 -59 42	3.73			
Inf Pariet Cortex	40	-38 -44 45	3.67	40	43 -35 39	4.22
Basal Ganglia		-8 -2 15	3.68			
Cingulate Cortex				31	19 -29 39	4.23
Cingulate Cortex				32	4 28 24	3.61
Cingulate Cortex				24	7 13 27	3.94
Precuneus				7	13 -68 39	4.27
Lingual Gyrus	17	-11 -92 -3	4.19	19	16 -62 0	4.38
Fusiform Gyrus	20	-35 -38 -18	3.49			
Fusiform Gyrus	20	-38 -26 -27	4.82	20	52 -23 -24	3.80
Uncus				28	25 -11 -30	4.07
Cerebellum		-8 -29 -18	3.77		43 -56 -39	3.65
Cerebellum		-44 -62 -45	4.15		16 -77 -45	4.30

References

Burgund ED, Kang HC, Kelly JE, Buckner RL, Snyder AZ, Petersen SE, Schlaggar BL. 2002. The Feasibility of a Common Stereotactic Space for Children and Adults in fMRI Studies of Development. *NeuroImage*. 17: 184-200.

Smith SM, Jenkinson M, Johansen-Berg H, Rueckert D, Nichols TE, Mackay CE, Watkins KE, Ciccarelli O, Cader MZ, Matthews PM, Behrens TEJ. 2006. Tract-based spatial statistics: Voxelwise analysis of multi-subject diffusion data. *NeuroImage*. 31: 1487-1505.

Yuan W, Altaye M, Ret J, Schmidthorst V, Byars AW, Plante E, Holland SK. 2009. Quantification of Head Motion in Children During Various fMRI Language Tasks. *Human Brain Mapping*. 30: 1481-1489.